



Oscillatory Flow of Couple Stress Fluid Flow over a Contaminated Fluid Sphere with Slip Condition

Parasa Naga Lakshmi Devi¹, Phani Kumar Meduri^{2,*}

¹ Department of Mathematics, Institute of Aeronautical Engineering, Dundigal, Hyderabad 500043, Telangana, India

² Department of Mathematics, School of Advanced Sciences, VIT-AP University, Amaravati, Andhra Pradesh, India

ARTICLE INFO

Article history:

Received 29 December 2022

Received in revised form 1 January 2023

Accepted 3 February 2023

Available online 1 August 2023

Keywords:

Couple stress fluid; viscous fluid; slip condition; surfactant; drag force; oscillatory flow

ABSTRACT

This research paper aims at finding the analytic solution for an oscillatory flow of couple stress fluid flow over a contaminated fluid sphere, filled with a couple stress fluid which is considered with interfacial slip on the boundary. The stream functions and drags related to the findings were analytically obtained. The special cases as a result of this are deduced for drag force which satisfies with the available data mentioned in the literature. The numerical values that were obtained are represented in both tabular and graphical forms for ease of representation. It has also been observed that in the case of viscous fluid, there is an inverse relation between real drag, slip parameter and viscosity ratio. It was also found that, there is a direct relation between imaginary drag, slip parameter and viscosity ratio respectively. For instance, in the case of the couple stress fluid, at lower values of the couple stress parameter there is a reduction in real drag, and an increase in imaginary drag respectively. These findings can result in future research considering body forces and other non-Newtonian fluids.

1. Introduction

Generally mass flow rate of a fluid affected by the solid particles (contaminants), presented in the form of bubbles and drops. The mass transfer of fluid flows between different places depends on many factors. The bubbles column observed in many industrial applications such as chemical, biochemical, wastewater treatment, food and pharmaceutical industries were reported by Asgharpour *et al.*, [1], and Nalajala & Kishore [2].

Ashmawy [3] developed mathematical equation which is used to study the behaviour of viscous fluids, subjected to torque was analysed by general Laplace transform technique applied on sphere. Happel and Brenner [4] described about the slip condition in their monograph.

Sherief & El-Sapa [5] considered the slow oscillatory motion of a spherical particle immersed in a fluid with a semi-infinite viscosity that is enclosed by an impermeable plane wall using no-slip kinematic condition and analytically evaluated its drag force. Faltas & El-Sapa [6] studied the

* Corresponding author.

E-mail address: phanikumarmeduri@gmail.com (Phani Kumar Meduri)

rectilinear oscillations of two spherical particles at low Reynolds number by using the collocation method. Rao & Rao [7] described the rectilinear and rotary oscillatory flows behaviour on a sphere along the diameter at no-slip condition. The couple of rotatory flow and drag by rectilinear oscillations are computed analytically. Charya & Iyengar [8] in their work, analyzed the effect of micro-polarity, frequency and geometric parameters on drag experienced by oscillatory flows on sphere and spheroidal shaped bodies.

Sadhal & Johnson [9] studied the creeping flow through a drop or a bubble of liquid, which has partly contaminated interfaces in an insoluble fluid which experiences the drag force. Vasconcelos *et al.*, [10] considered the effect of different bubble contractors on mass transfer coefficients. The work revealed the results of bubble contamination and sudden surface transition influence on the mass transfer when it reaches a stationary condition. Alves *et al.*, [11] developed the simplified static cap model used to express both gas-liquid mass transfers and drag coefficient in terms of bubble contamination kinetics. Kishore *et al.*, [12] have considered power law fluid flow over a moving liquid drop at intermediate Reynold numbers. They resolved the continuity and momentum equations using a simplified marker and cell (SMAC) algorithm developed based on the finite difference method. Saboni *et al.*, [13] in their study observed the flow significantly effected both the Reynold number and the static cap segment. They also investigated the coefficient of drag, which, under the conditions of a stable static cap and a specific viscosity ratio, is inversely proportional to Reynolds number. Saboni *et al.*, [14] conducted a numerical study to find the contamination effects on mass transfer of a fluid sphere, whose viscosity ratio was considered between dispersed and continuous phases. Additionally, their work discussed how the static cap angle affected mass transfer from the fluid sphere to the surrounding fluid for all Peclet numbers. Sharanya *et al.*, [15] in their work concluded about the effect of droplet movement in stretching and shrinkage condition. The analytical results clearly show that, a droplet migration velocity is mainly depended on thermal gradients. The behaviour of thermo-capillary stresses and the surfactant contaminates on the surface of a viscous spherical droplet was critically analysed. Ramana & Kumar [16], and Murthy & Kumar [17], respective works reported the estimating stream and vorticity functions for Stokes viscous uniform flow past a partially surfactant contaminated fluid sphere with slip and no-slip boundary conditions respectively. Kunche *et al.*, [18,19] obtained exact solution for uniform flow of micropolar fluid past a contaminated fluid drop and liquid drop with slip condition over the surface respectively.

Maiti & Misra [20] investigated how the particle size effects the physiological flow of blood in the microcirculatory system. The analytical and numerical analysis were done to study the effect of various parameters on physiological flow having high wavelength and small Reynold number. Akbar *et al.*, [21] investigated the effects of radiation and thermal diffusion on the mixed convection flow of couple stress fluid through a channel. The similarity transformation function was used to govern and transform the non-linear partial differential equations into ordinary differential equations. Shehadeh & Ashmawy [22] discussed about the influence of a non-dimensional torque on a couple stress fluid flow past a spherical surface with rotary oscillations over it. Prasad *et al.*, [23] developed a mathematical model to study the behaviour of blood flow between two layers comprising of core and peripheral regions. Assumptions also made that, core region fluid has couple stress fluid (CSF) with nanoparticles and peripheral region fluids are considered as Newtonian fluids. Rahul [24] discussed about the effect of various parameters on thermal instability of a couple stress fluid. The analytical method was used to obtain the solution. Devi *et al.*, [25,26], have obtained an exact solution for CSF flow beyond a fluid drop filled with a CSF and a partially contaminated non-Newtonian fluid sphere using with a slip condition and illustrated the drag force analytically.

Palaiah *et al.*, [27] investigated about the effect of dissipative free convection couple stress fluid flow over a cylinder under the action of magnetic field, thermal radiation and porous medium. Kumar

et al., [28] developed the couple stress model useful in converting the governing partial differential equations into non-linear ordinary differential equations with suitable boundary conditions. Muhammed *et al.*, [29] discussed on impact of squeezing flows which finds numerous applications in biological, mechanical and medical engineering. Reddy *et al.*, [30,31], work reported on unsteady hydro-magnetic CSF flow passed in a vertical cylinder was analyzed using the thermodynamic concept. Basha *et al.*, [32] developed couple stress liquid circulation equations over a vertical cylinder which were computationally solved by using the finite difference technique.

Narla *et al.*, [33,34], developed a mathematical model to analyze the micro polar fluid flows in heat transfer applications. Akram *et al.*, [35-37], reported works about the electro-osmotic based flows were analyzed with their developed mathematical models. Bhandari *et al.*, [38-40], discussed about the kinematics of the membrane-based flow model and their pumping characteristics were discussed. Ram *et al.*, [41] to demonstrate the viscoelastic nature of saliva, the Jeffrey fluid model is taken into consideration. Analytical solutions are chosen under the assumption that the flow is creeping and has a long wavelength and low Reynolds number.

Lu *et al.*, [42] developed a mathematical model which was used to study the electro-osmotic flows found in curved micro-vessels. Tripathi *et al.*, [43] present study, therefore, aims to investigate how temperature may affect virus transmission in peristaltic blood vessels and, furthermore, how virus density and particle diameter will affect the transmission of the virus from an infected person to a non-infected person. Shaw *et al.*, [44] analytically, the Bessel function is used to solve the governing equations for blood flow and the motion of magnetic nanoparticles.

The available literature focused mainly on oscillating flows, contaminated fluid sphere and couple stress fluid on different geometries with slip and no-slip conditions. The mentioned works have not addressed much on rectilinear oscillation of a couple stress fluid flows on a surfactant (contaminated) fluid sphere with slip condition. The present work mainly focuses on how to obtain an analytical solution for industrial applications, found in different categories of flows likely oscillatory flow of viscous fluid flow over a contaminated fluid sphere and oscillatory flow of couple stress fluid flow over a contaminated fluid sphere. Hence, the combination of couple stress fluid flow with contaminants is the new study. This study fills the research gap and it shows the new directions to the researchers to work more in this area.

The paper is organised as follows:

- I. Oscillatory flow of viscous fluid flow over a contaminated viscous fluid sphere.
- II. Oscillatory flow of couple stress fluid flow past a contaminated couple stress fluid sphere.

2. Methodology

2.1 Oscillatory Flow of Viscous Fluid Flow Over a Contaminated Viscous Fluid Sphere

2.1.1 Formulation of the problem

Consider an oscillatory flow of viscous fluid flow over a contaminated fluid sphere that is fixed in a stream of viscous fluid. The flow is assumed to be axisymmetric and incompressible. The surfactants (contamination) in the flow are accumulated at the rare end forming a cap region. x_0 is a varying point in between -1 to 1. The region which is contaminated is known as cap region ($x_0 < x \leq 1$) and the remaining portion ($-1 < x \leq x_0$) is no cap region. Geometry is given in Figure 1:

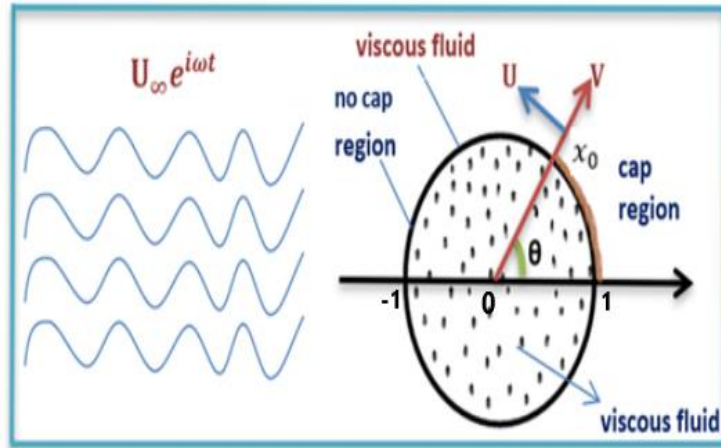


Fig. 1. Geometry of oscillatory viscous fluid flow over a contaminated viscous fluid sphere

The governing equations for the flow of an incompressible viscous fluid with no body forces are, continuity equation:

$$\frac{\partial \rho}{\partial t} + \nabla \cdot (\rho \bar{q}) = 0 \quad (1)$$

and the momentum equation:

$$\rho \frac{d\bar{q}}{dt} = -\nabla P + \mu(\nabla \times \nabla \times \bar{q}) \quad (2)$$

Due to the geometrical shape of the present problem, we choose spherical coordinate system for reference. The scale factors for the system are, $h_1 = 1$, $h_2 = R$, $h_3 = R \sin\theta$. Spherical coordinate system with origin at the center of the sphere and Z-axis along the flow direction is considered.

In axisymmetric flow the velocity components U, V are expressed as

$$U(r, \theta) = \frac{1}{R^2 \sin\theta} \frac{\partial \Psi}{\partial \theta}; \quad V(r, \theta) = \frac{-1}{R \sin\theta} \frac{\partial \Psi}{\partial R}.$$

Velocity field suitable for this oscillating flow are considered in the form,

$$\bar{q} = \nabla \times \left(\frac{\Psi \bar{e}_\theta}{h_3} \right) e^{i\omega t} = \left(\frac{1}{R^2 \sin\theta} \frac{\partial \Psi}{\partial \theta} \bar{e}_r - \frac{-1}{R \sin\theta} \frac{\partial \Psi}{\partial R} \bar{e}_\theta \right) e^{i\omega t}. \quad (3)$$

$$\therefore \nabla \times \bar{q} = - \left(\frac{E_0^2 \Psi}{h_3} \right) \bar{e}_\theta e^{i\omega t}; \quad (4)$$

Where, p is hydro-static pressure at any point, ρ is the fluid density, \bar{q} is the fluid velocity, μ is viscosity co-efficient, \bar{f} is body force per unit mass, η is couple stress viscosity coefficient, γ_1, γ_2 are roots of the given equation for stream functions, U_∞ is velocity at infinity, ω is oscillation frequency parameter, e is couple stress parameter, t is time.

Eliminating pressure P and Eq. (2) reduces to

$$E_0^2 \left[E_0^2 - \frac{\gamma_1^2}{a^2} \right] \Psi(r, \theta) = 0, \quad \text{where } E_0^2 \equiv \frac{\partial^2}{\partial R^2} + \frac{1}{R^2} \frac{\partial^2}{\partial \theta^2} - \frac{\cot\theta}{R^2} \frac{\partial}{\partial \theta}. \quad (5)$$

The non-dimensional scheme is taken as

$$R = ar; \Psi = \psi U_\infty a^2; P = p \frac{U_\infty \mu}{a}; E_0^2 = \frac{E^2}{a^2}; U = u U_\infty; V = v V_\infty$$

Using above in Eq. (5) reduces to

$$E^2[E^2 - \gamma_1^2] \psi(r, \theta) = 0, \tag{6}$$

where $E^2 \equiv \frac{\partial^2}{\partial r^2} + \frac{1}{r^2} \frac{\partial^2}{\partial \theta^2} - \frac{\cot \theta}{r^2} \frac{\partial}{\partial \theta}$, $\gamma_1^2 = \frac{i\rho\omega}{\eta}$. With $x = \cos \theta$, we get $E^2 \equiv \frac{\partial^2}{\partial r^2} + \frac{1-x^2}{r^2} \frac{\partial^2}{\partial x^2}$.

The solutions of ψ which are regular for external no-cap flow $\psi_{en} (-1 < x \leq x_0)$, internal no-cap flow $\psi_{in} (-1 < x \leq x_0)$ and external cap flow $\psi_{ec} (x_0 < x \leq 1)$, internal cap flow $\psi_{ic} (x_0 < x \leq 1)$ regions (by the method of separation of variables) are [16]:

$$\psi_e(r, x) = \begin{cases} \psi_{en}(r, x)G_2(x), & \text{for } -1 < x \leq x_0 \text{ (no - cap region)} \\ \psi_{ec}(r, x)G_2(x), & \text{for } x_0 < x \leq 1 \text{ (cap region)} \end{cases} \tag{7}$$

$$\psi_i(r, x) = \begin{cases} \psi_{in}(r, x)G_2(x), & \text{for } -1 < x \leq x_0 \text{ (no - cap region)} \\ \psi_{ic}(r, x)G_2(x), & \text{for } x_0 < x \leq 1 \text{ (cap region)} \end{cases} \tag{8}$$

2.1.2 Solution of the problem

The solutions of Eq. (6) which are regular for external flow of cap and no cap regions are (ψ'_{ec} & ψ'_{en}) and for internal flow of cap and no cap regions are (ψ'_{ic} & ψ'_{in}) given by:

$$\psi'_{en} = \left[r^2 + \frac{b_1}{r} + c_1 \sqrt{r} K_{\frac{3}{2}}(\gamma_{1en} r) \right] G_2(x) \tag{9}$$

$$\psi'_{in} = \left[b_2 r^2 + c_2 \sqrt{r} I_{\frac{3}{2}}(\gamma_{1in} r) \right] G_2(x) \tag{10}$$

$$\psi'_{ec} = \left[r^2 + \frac{b_3}{r} + c_3 \sqrt{r} K_{\frac{3}{2}}(\gamma_{1ec} r) \right] G_2(x) \text{ and} \tag{11}$$

$$\psi'_{ic} = \left[b_4 r^2 + c_4 \sqrt{r} I_{\frac{3}{2}}(\gamma_{1ic} r) \right] G_2(x) \tag{12}$$

where $K_{\frac{3}{2}}(x)$ and $I_{\frac{3}{2}}(x)$ are modified Bessel's functions of order $\frac{3}{2}$ and $G_2(x) = \frac{1}{2} (1 - x^2)$ is Gegenbauer polynomial of order 2.

In a cap region $b_4 = c_4 = 0$ i.e., $\psi'_{ic} = 0$. The parameters $b_1, c_1, b_2, c_2, b_3, c_3$ are obtained by implementing the following boundary conditions on Eq. (9) - Eq. (12).

I. Regularity conditions:

$$\begin{aligned}
 & a) \lim_{r \rightarrow \infty} \psi'_e = \frac{1}{2} r^2 \sin^2 \theta \text{ (outside the region)} \\
 & b) \lim_{r \rightarrow 0} \psi'_i = \text{Finite (inside the region)}
 \end{aligned} \tag{13}$$

II. Impermeability condition: on the boundary Normal velocity is zero.

$$\psi'_{en} = \psi'_{ec} = \psi'_{in} = \psi'_{ic} = 0, \text{ on } r = 1 \tag{14}$$

III. Slip condition: Tangential velocity is proportional to the tangential shear along the clear surface, i.e, [4,18]

$$\tau_{r\theta e} = \varepsilon(q_\theta - V_{\theta i}). \tag{15}$$

IV. Shear stress continuous at the interface of the fluid sphere i.e.,

$$\tau_{r\theta e} = \tau_{r\theta i}. \tag{16}$$

Using the boundary condition of Eq. (13) to Eq. (16) equations substituted in Eq. (9) to Eq. (12), the following system of equations were obtained

$$\begin{aligned}
 b_1 &= -1 - c'_1, \\
 b_2 &= -c'_2, \\
 b_3 &= -1 - c'_3, \\
 b_1(4 + s) + (c'_1)(2 + \gamma_{1en}^2 + (2 + s)\Delta_1(\gamma_{1en})) + 2sb_2 - sc'_2\Delta_2(\gamma_{1in}) &= 2s + 2; \\
 4b_1 + c'_1(2 + \gamma_{1en}^2 + 2\Delta_1(\gamma_{1en})) - \mu(-2b_2 + c'_2(2 + \gamma_{1in}^2 + 2\Delta_2(\gamma_{1in}))) &= 2; \\
 b_3(2 + s - \gamma_{1en}^2 - (2 + s)\Delta_1(\gamma_{1en})) - \gamma_{1ec}^2 - (2 + s)\Delta_3(\gamma_{1ec}) &= 2s + 4;
 \end{aligned} \tag{17}$$

Where, $c'_1 = c_1 K_{\frac{3}{2}}(\gamma_{1en})$; $c'_2 = c_2 I_{\frac{3}{2}}(\gamma_{1in})$; $c'_3 = c_3 K_{\frac{3}{2}}(\gamma_{1ec})$, slip parameter $= s = \frac{\varepsilon a}{\mu}$, viscosity ratio $\mu = \frac{\mu_i}{\mu_e}$.

Solving Eq. (17) analytically, resulted to

$$b_1 = \frac{(2s+4+\gamma_{1en}^2+(2+s)\Delta_1(\gamma_{1en}))q'_2 - (4+\gamma_{1en}^2+2\Delta_1(\gamma_{1en}))j'_2}{\phi'};$$

$$b_2 = \frac{(4 + \gamma_{1en}^2 + 2\Delta_1(\gamma_{1en}))j_1' - (2s + 4 + \gamma_{1en}^2 + (2+s)\Delta_1(\gamma_{1en}))q_1'}{\phi'};$$

$$b_3 = \frac{2s + 4 + \gamma_{1ec}^2 + (2+s)\Delta_3(\gamma_{1ec})}{j_3'};$$

where, $\phi' = j_1'q_2' - j_2'q_1'$,

$$j_1' = [s + 2 - \gamma_{1en}^2 - (2 + s)\Delta_1(\gamma_{1en})];$$

$$j_2' = s [\Delta_2(\gamma_{1in}) + 2];$$

$$q_1' = [-\gamma_{1en}^2 - 2\Delta_1(\gamma_{1en}) + 2];$$

$$q_2' = \mu[4 + \gamma_{1in}^2 + 2\Delta_2(\gamma_{1in})];$$

$$j_3' = [s + 2 - \gamma_{1ec}^2 - (2 + s)\Delta_3(\gamma_{1ec})].$$

Thus, external and internal flow stream functions are derived.

2.1.3 Drag force on a fluid sphere

The drag force in limit form on a body, which is placed in an oscillatory flow, is

$$D_g = i\rho\omega UV + 4\pi i\rho\omega \lim_{r \rightarrow \infty} \left[\frac{r(\psi_e' - \psi_\infty^*)}{\sin^2 \theta} \right] e^{i\omega t}. \quad (18)$$

Where, ψ_∞^* denotes the stream function correlate with the fluid motion at infinity [4]. D_g is drag force, θ is real drag coefficient, θ_1 is imaginary drag coefficient.

Substituting Eq. (9), Eq. (11), Eq. (13) and $V = \frac{4}{3}\pi r^3$ in Eq. (18) we get,

$$\begin{aligned} D_g &= \frac{4}{3}\pi i\rho\omega e^{i\omega t} ((b_1 + c_1' + 1) + (b_3 + c_3' + 1)) + 2\pi i\rho\omega e^{i\omega t} (b_1 + b_3), \\ &= 2\pi i\rho\omega e^{i\omega t} (b_1 + b_3), \text{ (since using Eq. (17))} \end{aligned} \quad (19)$$

$$= -2\pi i\rho\omega (i\theta + \theta_1)(b_1 + b_3)e^{i\omega t}. \quad (20)$$

with $\mu \rightarrow \infty$, $s \rightarrow \infty$ oscillatory viscous flow on the solid sphere with no-slip condition results are obtained, which correlate to the results of Lakshmana Rao & Rao [7].

In addition, we have obtained drag force of oscillatory flow of couple stress fluid flow past a contaminated couple stress fluid sphere.

2.2 Oscillatory Flow of Couple Stress Fluid Flow Past a Contaminated Couple Stress Fluid Sphere

2.2.1 Formulation of the problem

Consider a contaminated fluid sphere with couple stress fluid inside it, is placed in an oscillatory couple stress fluid flow with a uniform velocity far away from it. The flow is assumed incompressible,

and axisymmetric. Geometry is given in Figure 2.

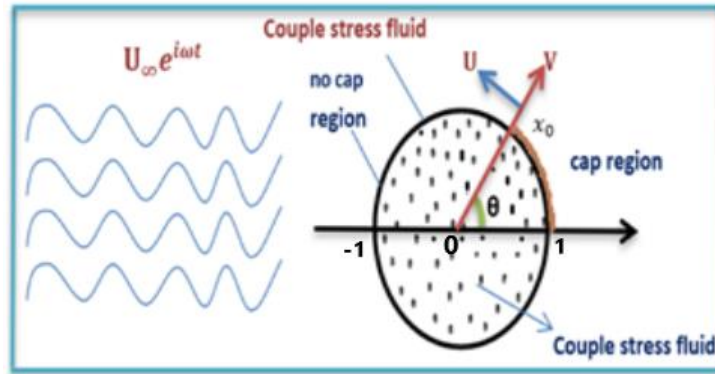


Fig. 2. Flow geometry of oscillatory CSF flow over a contaminated couple stress fluid sphere

The field equations that determine couple stress fluid flow with no body forces is as follows:

$$\rho \frac{d\bar{q}}{dt} = -\nabla P + \mu(\nabla \times \nabla \times \bar{q}) - \eta(\nabla \times \nabla \times \nabla \times \bar{q}). \quad (21)$$

Here \bar{q} is the fluid velocity, p is the pressure, ρ is the density and μ, η are viscosity and couple stress viscosity coefficients.

Velocity of oscillating flow are considered in the form,

$$\bar{q} = \nabla \times \left(\frac{\Psi \bar{e}_\theta}{h_3} \right) e^{i\omega t} = \left(\frac{1}{R^2 \sin\theta} \frac{\partial \Psi}{\partial \theta} \bar{e}_r - \frac{-1}{R \sin\theta} \frac{\partial \Psi}{\partial R} \bar{e}_\theta \right) e^{i\omega t}. \quad (22)$$

$$\therefore \nabla \times \bar{q} = - \left(\frac{E_0^2 \Psi}{h_3} \right) \bar{e}_\theta e^{i\omega t}; \quad \nabla \times \nabla \times \nabla \times \bar{q} = - \left(\frac{E_0^4 \Psi}{h_3} \right) \bar{e}_\theta e^{i\omega t}. \quad (23)$$

Eliminating pressure P and reduces to Eq. (21) we get

$$\frac{1}{R} \frac{\partial P}{\partial \theta} = \frac{\mu}{R \sin\theta} \frac{\partial(E_0^2 \Psi)}{\partial R} - \frac{\eta}{R \sin\theta} \frac{\partial(E_0^4 \Psi)}{\partial R}. \quad (24)$$

After eliminating the pressure P , from Eq. (21) we get

$$E_0^2 \left[E_0^2 - \frac{\gamma_1^2}{a^2} \right] \left[E_0^2 - \frac{\gamma_2^2}{a^2} \right] \Psi(r, \theta) = 0, \quad (25)$$

$$\text{where } \gamma_1^2 + \gamma_2^2 = \frac{\mu a^2}{\eta}; \quad \gamma_1^2 \gamma_2^2 = \frac{i \rho \omega a^4}{\eta}.$$

The following non-dimensional scheme is taken.

$$R = ar; \quad \Psi = \psi U_\infty a^2; \quad P = p \frac{U_\infty \mu}{a}; \quad E_0^2 = \frac{E^2}{a^2}; \quad U = u U_\infty; \quad V = v V_\infty.$$

The momentum equation of non-dimensional form is

$$E^2[E^2 - \gamma_1^2][E^2 - \gamma_2^2]\psi(r, \theta) = 0 \quad (26)$$

where $E^2 \equiv \frac{\partial^2}{\partial r^2} + \frac{1}{r^2} \frac{\partial^2}{\partial \theta^2} - \frac{\cot \theta}{r^2} \frac{\partial}{\partial \theta}$.

With $x = \cos \theta$, we get $E^2 \equiv \frac{\partial^2}{\partial r^2} + \frac{1-x^2}{r^2} \frac{\partial^2}{\partial x^2}$

The solution of Eq. (26) by variable separable method, which are regular for external flow (ψ_e) and for internal flow (ψ_i) regions by super position process are given by:

$$\psi_{en}(r, x) = \left[r^2 + \frac{b_1}{r} + c_1 \sqrt{r} K_{\frac{3}{2}}(\gamma_{1en} r) + d_1 \sqrt{r} K_{\frac{3}{2}}(\gamma_{2en} r) \right] G_2(x), \quad (27)$$

$$\psi_{in}(r, x) = \left[b_2 r^2 + c_2 \sqrt{r} I_{\frac{3}{2}}(\gamma_{1in} r) + d_2 \sqrt{r} I_{\frac{3}{2}}(\gamma_{2in} r) \right] G_2(x), \quad (28)$$

$$\psi_{ec}(r, x) = \left[r^2 + \frac{b_3}{r} + c_3 \sqrt{r} K_{\frac{3}{2}}(\gamma_{1ec} r) + d_3 \sqrt{r} K_{\frac{3}{2}}(\gamma_{2ec} r) \right] G_2(x), \quad (29)$$

$$\psi_{ic}(r, x) = \left[b_4 r^2 + c_4 \sqrt{r} I_{\frac{3}{2}}(\gamma_{1ic} r) + d_4 \sqrt{r} I_{\frac{3}{2}}(\gamma_{2ic} r) \right] G_2(x). \quad (30)$$

In a cap region, $b_4 = c_4 = d_4 = 0$, then $\psi_{ic} = 0$. The parameters $b_1, c_1, d_1, b_2, c_2, d_2, b_3, c_3, d_3$, are obtained by implementing the following boundary conditions:

I. Regularity conditions:

a) $\lim_{r \rightarrow \infty} \psi_e = \frac{1}{2} r^2 \sin^2 \theta$ (outside the region) (31)

b) $\lim_{r \rightarrow 0} \psi_i = \text{Finite}$ (inside the region).

II. Impermeability condition: on the boundary Normal velocity is zero.

$$\psi_{en} = \psi_{ec} = \psi_{in} = \psi_{ic} = 0, \text{ on } r = 1. \quad (32)$$

III. Slip condition: Tangential velocity is proportional to the tangential shear along the clear surface, i.e., [4,18]

$$\tau_{r\theta e} = \varepsilon(q_\theta - V_{\theta i}) \quad (33)$$

IV. Shear stress continuous at the interface of the fluid sphere i.e.,

$$\tau_{r\theta e} = \tau_{r\theta i}. \quad (34)$$

V. Type A (Hyper-stick) condition: Couple stresses on the sphere $r = 1$ should vanish. Impermeability condition: on the boundary Normal velocity is zero.

$$\frac{\partial[E^2\psi]}{\partial r} = \left(\frac{1}{r} + e\right) E^2\psi \text{ where } e = \frac{\eta'}{\eta} \text{ is couple stress parameter.} \quad (35)$$

Using the boundary conditions (Eq. (31) to Eq. (35)) in Eq. (27) to Eq. (30) we get the following nine system of equations,

$$\begin{aligned}
 & b_1 + c'_1 + d'_1 = -1; \\
 & b_2 + c'_2 + d'_2 = 0; \\
 & b_3 + c'_3 + d'_3 = -1; \\
 & b_1(6 + s) + c'_1 \left(\gamma_{1en}^2 + 4 + (2 + s)\Delta_1(\gamma_{1en}) - \frac{\gamma_{1en}^4}{\lambda^2} \right) + d'_1 \left(\gamma_{2en}^2 + 4 + (2 + s)\Delta_1(\gamma_{2en}) - \frac{\gamma_{2en}^4}{\lambda^2} \right) \\
 & + 2sb_2 - s c'_2 \Delta_2(\gamma_{1in}) - d'_2 s \Delta_2(\gamma_{2in}) = 2s; \\
 & b_3(6 + s) + c'_3 \left(\gamma_{1ec}^2 + 4 + (2 + s)\Delta_3(\gamma_{1ec}) - \frac{\gamma_{1ec}^4}{\lambda^2} \right) + d'_3 \left(\gamma_{2ec}^2 + 4 + (2 + s)\Delta_3(\gamma_{2ec}) - \frac{\gamma_{2ec}^4}{\lambda^2} \right) \\
 & = 2s; \\
 & 6b_1 + c'_1 \left(4 + \gamma_{1en}^2 + 2\Delta_1(\gamma_{1en}) - \frac{\gamma_{1en}^4}{\lambda^2} \right) + d'_1 \left(4 + \gamma_{2en}^2 + 2\Delta_1(\gamma_{2en}) - \frac{\gamma_{2en}^4}{\lambda^2} \right) - \\
 & \mu c'_2 \left(4 + \gamma_{1in}^2 + 2\Delta_2(\gamma_{1in}) - \frac{\gamma_{1in}^4}{\lambda^2} \right) - \mu d'_2 \left(4 + \gamma_{2in}^2 + 2\Delta_2(\gamma_{2in}) - \frac{\gamma_{2in}^4}{\lambda^2} \right) = 0 \\
 & \gamma_{1en}^2 c'_1 \{ \Delta_1(\gamma_{1en}) + (1 + e) \} + \gamma_{2en}^2 d'_1 \{ \Delta_1(\gamma_{2en}) + (1 + e) \} = 0; \\
 & \gamma_{1in}^2 c'_2 \{ \Delta_2(\gamma_{1in}) + (1 + e) \} + \gamma_{2in}^2 d'_2 \{ \Delta_2(\gamma_{2in}) + (1 + e) \} = 0 \\
 & ; \\
 & \gamma_{1ec}^2 c'_3 \{ \Delta_3(\gamma_{1ec}) + (1 + e) \} + \gamma_{2ec}^2 d'_3 \{ \Delta_3(\gamma_{2ec}) + (1 + e) \} = 0;
 \end{aligned} \tag{36}$$

Where, $c'_1 = c_1 K_{\frac{3}{2}}(\gamma_{1en})$, $c'_2 = c_2 I_{\frac{3}{2}}(\gamma_{1in})$, $c'_3 = c_3 K_{\frac{3}{2}}(\gamma_{1ec})$, $d'_1 = d_1 K_{\frac{3}{2}}(\gamma_{2en})$, $d'_2 = d_2 I_{\frac{3}{2}}(\gamma_{2in})$, and $d'_3 = d_3 K_{\frac{3}{2}}(\gamma_{2ec})$; slip parameter $s = \frac{\varepsilon a}{\mu}$, viscosity ratio $\mu = \frac{\mu_i}{\mu_e}$, $e = \frac{\eta'}{\eta}$; with $(\eta' \neq \eta)$.

Solving Eq. (36), we get

$$b_1 = -1 + (\zeta_1 - 1)d'_1, \quad c'_1 = -\zeta_1 d'_1 \quad \text{and} \quad d'_1 = \frac{-(3s+6)q'_4 + 6j'_5}{\phi};$$

$$b_2 = (\zeta_2 - 1)d'_2, \quad c'_2 = -\zeta_2 d'_2 \quad \text{and} \quad d'_2 = \frac{(3s+6)q'_3 - 6j'_4}{\phi};$$

$$b_3 = -1 + (\zeta_3 - 1)d'_3, \quad c'_3 = -\zeta_3 d'_3 \quad \text{and} \quad d'_3 = \frac{3s+6}{j'_6};$$

$$\zeta_1 = \frac{\gamma_{2en}^2[\Delta_1(\gamma_{2en})+(1+e)]}{\gamma_{1en}^2[\Delta_1(\gamma_{1en})+(1+e)]}, \zeta_2 = \frac{\gamma_{2in}^2[\Delta_2(\gamma_{2in})+(1+e)]}{\gamma_{1in}^2[\Delta_2(\gamma_{1in})+(1+e)]}, \zeta_3 = \frac{\gamma_{2ec}^2[\Delta_3(\gamma_{2ec})+(1+e)]}{\gamma_{1ec}^2[\Delta_3(\gamma_{1ec})+(1+e)]},$$

where, $\phi = j'_4 q'_4 - j'_5 q'_3$

$$j'_4 = \left[\zeta_1 \left(-2 - s + \gamma_{1en}^2 + (2 + s)\Delta_1(\gamma_{1en}) - \frac{\gamma_{1en}^4}{\lambda^2} \right) + s + 2 - \gamma_{2en}^2 - (2 + s)\Delta_1(\gamma_{2en}) + \frac{\gamma_{2en}^4}{\lambda^2} \right];$$

$$j'_5 = s [\zeta_2(-\Delta_2(\gamma_{1in}) - 2) + 2 + \Delta_2(\gamma_{2in})];$$

$$q'_3 = \left[\zeta_1 \left(\gamma_{1en}^2 + 2\Delta_1(\gamma_{1en}) - \frac{\gamma_{1en}^4}{\lambda^2} - 2 \right) + 2 - \gamma_{2en}^2 - 2\Delta_1(\gamma_{2en}) + \frac{\gamma_{2en}^4}{\lambda^2} \right];$$

$$q'_4 = \mu \left[\zeta_2 \left(-4 - \gamma_{1in}^2 - 2\Delta_2(\gamma_{1in}) + \frac{\gamma_{1in}^4}{\lambda^2} \right) + \gamma_{2in}^2 + 4 + 2\Delta_2(\gamma_{2in}) - \frac{\gamma_{2in}^4}{\lambda^2} \right];$$

$$j'_6 = \left[\zeta_3 \left(-2 - s + \gamma_{1ec}^2 + (2 + s)\Delta_3(\gamma_{1ec}) - \frac{\gamma_{1ec}^4}{\lambda^2} \right) + s + 2 - \gamma_{2ec}^2 - (2 + s)\Delta_3(\gamma_{2ec}) + \frac{\gamma_{2ec}^4}{\lambda^2} \right].$$

Thus, external and internal flow of stream functions is obtained.

2.2.2 Drag force on a sphere

The limit for the drag force on a body, which is placed in an oscillatory flow, is

$$D_g = i\rho\omega UV + 4\pi i\rho\omega \lim_{r \rightarrow \infty} \left[\frac{r(\psi'_e - \psi^*_\infty)}{\sin^2 \theta} \right] e^{i\omega t}, \quad (37)$$

where ψ^*_∞ denotes the stream function correlate to the fluid motion at infinity [4].

Substituting Eq. (27), Eq. (29), Eq. (31) and $V = \frac{4}{3}\pi r^3$ in Eq. (37) we get,

$$\begin{aligned} D_g &= \frac{4}{3}\pi i\rho\omega e^{i\omega t} ((b_1 + c'_1 + d'_1 + 1) + (b_3 + c'_3 + d'_3 + 1)) + 2\pi i\rho\omega e^{i\omega t} (b_1 + b_3), \\ &= 2\pi i\rho\omega e^{i\omega t} (b_1 + b_3), \text{ (since using Eq. (36))} \end{aligned} \quad (38)$$

$$= -2\pi i\rho\omega (i\theta + \theta_1)(b_1 + b_3)e^{i\omega t}. \quad (39)$$

with $\gamma_1 \rightarrow \infty$, $\gamma_2 \rightarrow \infty$, $\mu \rightarrow \infty$, $s \rightarrow \infty$ oscillatory viscous flow on the solid sphere with no-slip condition results are obtained, which correlate to the results of Lakshmana Rao & Rao [7].

3. Results and Discussion

3.1 Case 1: Oscillatory Flow of Viscous Fluid Flow Over a Contaminated Viscous Fluid Sphere

The internal and external stream functions of Eq. (9) to Eq. (12) are computed using the boundary conditions from (13) - (16). The drag force of viscous fluid past a contaminated viscous fluid is computed and is given in Eq. (20). Real drag and imaginary drag values are evaluated and its variations

related to varied slip parameter and viscosity ratio (μ) are presented in Figure 3 and Figure 4, at fixed values to frequency parameters $\mu = 10, \rho = 0.6, \omega = 0.6, t = 0.6$.

Real drag (θ) vs slip parameter (s) at different viscosity ratio (μ) values are plotted in Figure 3. It was noticed that with a rise in slip parameter (s) values there is a decrease in real drag (θ) and there is a decrease in the values of real drag (θ) with increase in values of viscosity ratio (μ). The numerical results are given in Table 1.

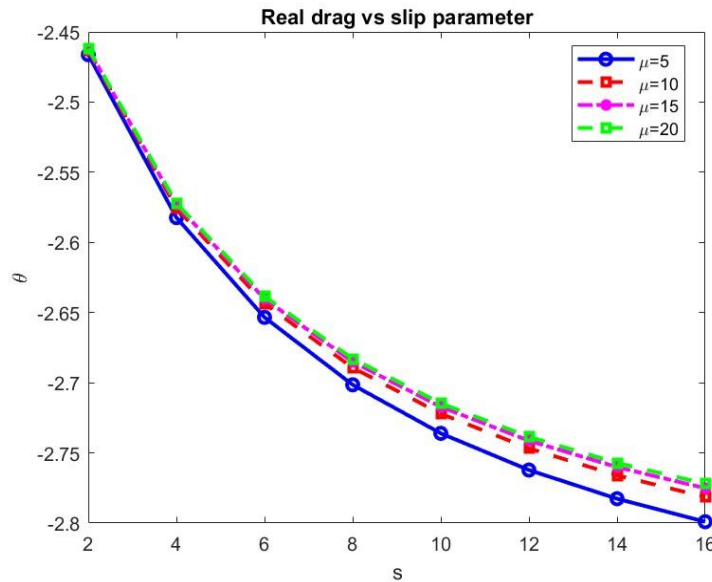


Fig. 3. Real drag (θ) vs slip parameter (s) for different viscosity ratio (μ) at fixed values to frequency parameters $\mu = 10, \omega = 0.6, \rho = 0.6, t = 0.6$

Table 1

Real drag (θ) vs slip parameter (s) for different viscosity ratio (μ) at fixed values to frequency parameters $\mu = 10, \omega = 0.6, \rho = 0.6, t = 0.6$

$s \backslash \mu$	5	10	15	20
2	-2.4662	-2.4633	-2.4623	-2.4617
4	-2.5823	-2.5755	-2.5732	-2.572
6	-2.6534	-2.6436	-2.6402	-2.6385
8	-2.7015	-2.6893	-2.6851	-2.6829
10	-2.7361	-2.7221	-2.7172	-2.7147
12	-2.7622	-2.7468	-2.7413	-2.7385
14	-2.7826	-2.766	-2.7601	-2.7571
16	-2.7991	-2.7814	-2.7752	-2.772

Imaginary drag (θ_1) vs slip parameter (s) at different viscosity ratio (μ) values are plotted in Figure 4. It was noticed that with rise in slip parameter (s) values there is rise in imaginary drag (θ_1) and there is an increase in the values of imaginary drag (θ_1) with a decrease in values of viscosity ratio (μ). The numerical results are given in Table 2.

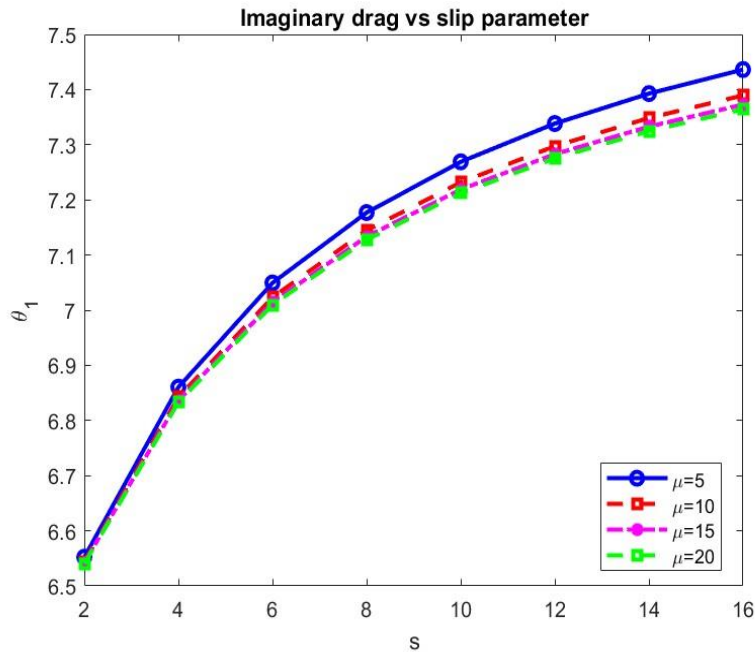


Fig. 4. Imaginary drag (θ_1) vs slip parameter (s) for different viscosity ratio (μ) at fixed values to frequency parameters $\mu = 10, \omega = 0.6, \rho = 0.6, t = 0.6$

Table 2

Imaginary drag (θ_1) vs slip parameter (s) for different viscosity ratio (μ) at fixed values to frequency parameters $\mu = 10, \omega = 0.6, \rho = 0.6, t = 0.6$

$s \backslash \mu$	5	10	15	20
2	6.5521	6.5443	6.5416	6.5394
4	6.8605	6.8425	6.8363	6.8313
6	7.0494	7.0234	7.0143	7.0069
8	7.177	7.1447	7.1335	7.1242
10	7.269	7.2318	7.2188	7.2081
12	7.3385	7.2974	7.2829	7.2711
14	7.3927	7.3485	7.3329	7.32
16	7.4363	7.3894	7.3729	7.3593

3.2 Case 2: Oscillatory Flow of Couple Stress Fluid Flow Past a Contaminated Couple Stress Fluid Sphere

The internal and external stream functions Eq. (27) to Eq. (30) are computed using the boundary conditions from Eq. (31) to Eq. (35). The drag force of couple stress fluid flow past a contaminated couple stress fluid is computed and is given in Eq. (39). Real drag (θ) and imaginary drag (θ_1) values are evaluated and its variations related to varied couple stress parameter and slip parameter values are presented in Figure 5 and Figure 6, at fixed values to frequency parameters $\mu = 10, \lambda = 0.258, \rho = 0.6, \omega = 0.6, t = 0.6$.

Real drag (θ) vs couple stress parameter (e) for different slip parameter (s) values are arranged in Figure 5. It was noticed that at lower values of couple stress parameter (e) i.e., less than 4 there is decrease in real drag (θ) values after that there is a slight increasing real drag values and there

after the values got stable. Also noticed that with rise in slip parameter (s) there is rise in real drag (θ) values. The numerical results are presented in Table 3.

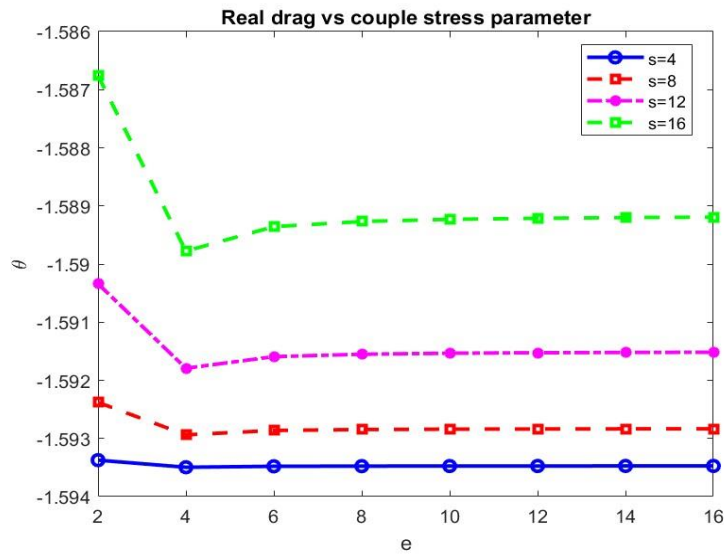


Fig. 5. Real drag (θ) vs couple stress parameter (e) for different slip parameter (s) at fixed values to frequency parameters $\mu = 10$, $\omega = 0.6$, $\rho = 0.6$, $\lambda = 0.258$, $t = 0.6$

Table 3

Real drag (θ) vs couple stress parameter (e) for different slip parameter (s) at fixed values to frequency parameters $\mu = 10$, $\omega = 0.6$, $\rho = 0.6$, $\lambda = 0.258$, $t = 0.6$

e/s	4	8	12	16
2	-1.5934	-1.5924	-1.5903	-1.5868
4	-1.5935	-1.5929	-1.5918	-1.5998
6	-1.5935	-1.5929	-1.5916	-1.5994
8	-1.5935	-1.5928	-1.5916	-1.5993
10	-1.5935	-1.5928	-1.5915	-1.5992
12	-1.5935	-1.5928	-1.5915	-1.5992
14	-1.5935	-1.5928	-1.5915	-1.5992
16	-1.5935	-1.5928	-1.5915	-1.5992

Imaginary drag (θ_1) vs couple stress parameter (e) for different slip parameter (s) values are arranged in Figure 6. It was noticed that at lower values of couple stress parameter (e) i.e., less than 4 there is rise in imaginary drag (θ_1) values after that there is a slight decrease in imaginary drag values. Also noticed that with rise in slip parameter (s) there is a decrease in imaginary drag (θ_1) values, there after the values are stable. The numerical results are presented in Table 4.

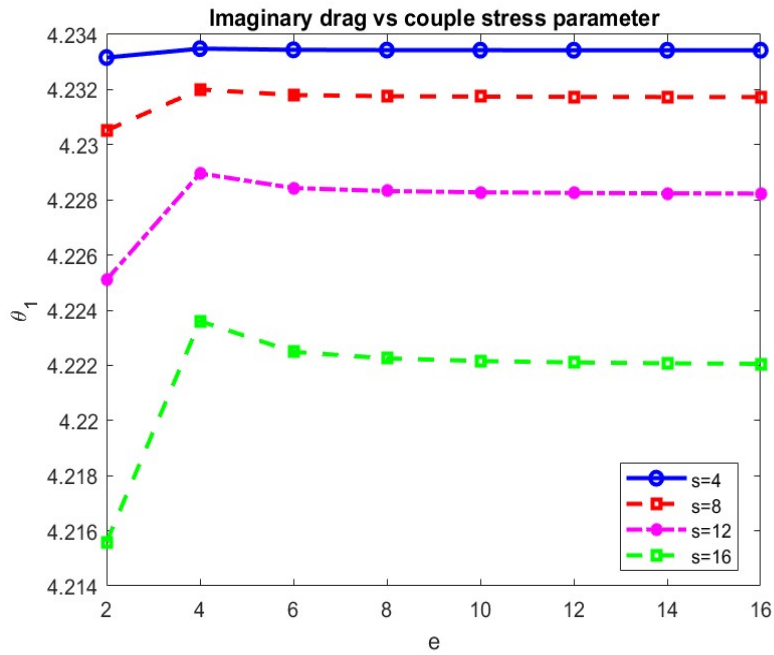


Fig. 6. Imaginary drag (θ_1) vs couple stress parameter (e) for different slip parameter (s) at fixed values to frequency parameters $\mu = 10, \omega = 0.6, \rho = 0.6, \lambda = 0.258, t = 0.6$

Table 4

Imaginary drag (θ_1) vs couple stress parameter (e) for different slip parameter (s) at fixed values to frequency parameters $\mu = 10, \omega = 0.6, \rho = 0.6, \lambda = 0.258, t = 0.6$

e/s	4	8	12	16
2	4.2332	4.2305	4.2251	4.2156
4	4.2335	4.232	4.229	4.2236
6	4.2334	4.2318	4.2284	4.2225
8	4.2334	4.2318	4.2283	4.2223
10	4.2334	4.2317	4.2283	4.2222
12	4.2334	4.2317	4.2283	4.2222
14	4.2334	4.2317	4.2282	4.2221
16	4.2334	4.2317	4.2282	4.2221

4. Conclusions

In this study we have obtained an exact solution for oscillatory couple stress fluid flow past a contaminated couple stress fluid sphere with slip condition on its surface. In addition to this, the exact solutions were also obtained for the oscillatory flow of viscous fluid flow over a contaminated viscous fluid sphere. The drag force for the above cases were solved analytically and results were validated for special cases. After thorough analysis the following observations were obtained:

In Viscous Fluid Case:

- I. there is an inverse relation between real drag (θ), slip parameter (s), viscosity ratio (μ) respectively.
- II. there is direct relation between imaginary drag (θ_1), slip parameter (s), viscosity ratio (μ) respectively.

In Couple Stress Fluid Case:

- I. at lower values of couple stress parameter (e) there is a reduce in real drag (θ), increase in imaginary drag (θ_1) respectively.

From the above-mentioned findings, it is evident that this study would be of relevance to the industry and academia.

Acknowledgement

This research was not funded by any grant

References

- [1] Asgharpour, Maryam, Mohammad Reza Mehrnia, and Navid Mostoufi. "Effect of surface contaminants on oxygen transfer in bubble column reactors." *Biochemical engineering journal* 49, no. 3 (2010): 351-360. <https://doi.org/10.1016/j.bej.2010.01.010>
- [2] Nalajala, Venkata Swamy, and Nanda Kishore. "Drag of contaminated bubbles in power-law fluids." *Colloids and Surfaces A: Physicochemical and Engineering Aspects* 443 (2014): 240-248. <https://doi.org/10.1016/j.colsurfa.2013.11.014>
- [3] Ashmawy, E. A. "Unsteady rotational motion of a slip spherical particle in a viscous fluid." *International Scholarly Research Notices* 2012 (2012). <https://doi.org/10.5402/2012/513717>
- [4] Happel, John, and Howard Brenner. "The behavior of fluids in slow motion." In *Low Reynolds number hydrodynamics*, pp. 23-57. Springer, Dordrecht, 1983. <https://doi.org/10.1007/978-94-009-8352-6>
- [5] Sherief, H. H., M. S. Faltas, and Shreen El-Sapa. "Force on a spherical particle oscillating in a viscous fluid perpendicular to an impermeable planar wall." *Journal of the Brazilian Society of Mechanical Sciences and Engineering* 41 (2019): 1-10. <https://doi.org/10.1007/s40430-019-1750-7>
- [6] Faltas, M. S., and Shreen El-Sapa. "Rectilinear oscillations of two spherical particles embedded in an unbounded viscous fluid." *Microsystem Technologies* 25, no. 1 (2019): 39-49. <https://doi.org/10.1007/s00542-018-3928-9>
- [7] Rao, SK Lakshmana, and P. Bhujanga Rao. "The oscillations of a sphere in a micropolar fluid." *International Journal of Engineering Science* 9, no. 7 (1971): 651-672. [https://doi.org/10.1016/0020-7225\(71\)90068-1](https://doi.org/10.1016/0020-7225(71)90068-1)
- [8] Charya, D. Srinivasa, and T. K. V. Iyengar. "Drag on an axisymmetric body performing rectilinear oscillations in a micropolar fluid." *International journal of engineering science* 35, no. 10-11 (1997): 987-1001. [https://doi.org/10.1016/S0020-7225\(97\)00103-1](https://doi.org/10.1016/S0020-7225(97)00103-1)
- [9] Sadhal, S. S., and Robert E. Johnson. "Stokes flow past bubbles and drops partially coated with thin films. Part 1. Stagnant cap of surfactant film—exact solution." *Journal of Fluid Mechanics* 126 (1983): 237-250. <https://doi.org/10.1017/S0022112083000130>
- [10] Vasconcelos, J. M. T., J. M. L. Rodrigues, S. C. P. Orvalho, S. S. Alves, R. L. Mendes, and A. Reis. "Effect of contaminants on mass transfer coefficients in bubble column and airlift contactors." *Chemical Engineering Science* 58, no. 8 (2003): 1431-1440. [https://doi.org/10.1016/S0009-2509\(02\)00675-9](https://doi.org/10.1016/S0009-2509(02)00675-9)
- [11] Alves, S. S., S. P. Orvalho, and J. M. T. Vasconcelos. "Effect of bubble contamination on rise velocity and mass transfer." *Chemical Engineering Science* 60, no. 1 (2005): 1-9. <https://doi.org/10.1016/j.ces.2004.07.053>
- [12] Kishore, N., R. P. Chhabra, and V. Eswaran. "Drag on a single fluid sphere translating in power-law liquids at moderate Reynolds numbers." *Chemical engineering science* 62, no. 9 (2007): 2422-2434. <https://doi.org/10.1016/j.ces.2007.01.057>
- [13] Saboni, A., S. Alexandrova, and M. Mory. "Flow around a contaminated fluid sphere." *International Journal of Multiphase Flow* 36, no. 6 (2010): 503-512. <http://dx.doi.org/10.1016/j.ijmultiphaseflow.2010.01.009>
- [14] Saboni, Abdallah, Silvia Alexandrova, Maria Karsheva, and Christophe Gourdon. "Mass transfer from a contaminated fluid sphere." *AIChE journal* 57, no. 7 (2011): 1684-1692. <https://doi.org/10.1002/aic.12391>
- [15] Sharanya, V., B. Sri Padmavati, and G. P. Raja Sekhar. "Transient Stokes flow past a spherical droplet with a stagnant cap due to contaminated surfactant layer." *Theoretical and Computational Fluid Dynamics* 35 (2021): 783-806. <https://doi.org/10.1017/jfm.2012.205>
- [16] Ramana Murthy, J. V., and M. Phani Kumar. "Drag over contaminated fluid sphere with slip condition." *International Journal of Scientific & Engineering Research* 5, no. 5 (2014): 719-727.
- [17] Murthy, JV Ramana, and M. Phani Kumar. "Exact solution for flow over a contaminated fluid sphere for Stokes flow." In *Journal of Physics: Conference Series*, vol. 662, no. 1, p. 012016. IOP Publishing, 2015. <http://dx.doi.org/10.1088/1742-6596/662/1/012016>

- [18] Kunche, Vijaya Lakshmi, and Phani Kumar MEDURI. "Exact Solution for Non-Newtonian Fluid Flow Beyond a Contaminated Fluid Sphere." *Engineering Transactions* 70, no. 3 (2022): 287-299. <https://doi.org/10.24423/EngTrans.1417.20220726>
- [19] Kunche, Vijaya Lakshmi, and Phani Kumar Meduri. "Stokes flow of Micropolar fluid beyond fluid sphere with slip condition." *ZAMM-Journal of Applied Mathematics and Mechanics/Zeitschrift für Angewandte Mathematik und Mechanik* 102, no. 11 (2022): e202100340. <https://doi.org/10.1002/zamm.202100340>
- [20] Maiti, S., and J. C. Misra. "Peristaltic transport of a couple stress fluid: some applications to hemodynamics." *Journal of Mechanics in Medicine and Biology* 12, no. 03 (2012): 1250048. <http://dx.doi.org/10.1142/S0219519411004733>
- [21] Akbar, Ajed, Hakeem Ullah, Muhammad Asif Zahoor Raja, Kottakkaran Sooppy Nisar, Saeed Islam, and Muhammad Shoaib. "A design of neural networks to study MHD and heat transfer in two phase model of nano-fluid flow in the presence of thermal radiation." *Waves in Random and Complex Media* (2022): 1-24. <http://dx.doi.org/10.18869/acadpub.jafm.68.224.22695>
- [22] Shehadeh, Tarek, and Emad Ashmawy. "Rotary Oscillation of a Rigid Sphere in a Couple Stress Fluid." *BAU Journal-Science and Technology* 1, no. 1 (2019): 8. <https://doi.org/10.54729/2959-331X.1009>
- [23] Prasad, K. Maruthi, N. Subadra, and B. Rama Krishna Reddy. "A mathematical study on two layered blood flow of a couple-stress fluid." In *AIP Conference Proceedings*, vol. 2246, no. 1, p. 020054. AIP Publishing LLC, 2020. <https://doi.org/10.1063/5.0014549>
- [24] Rahul, Naveen Sharma. "Thermal Instability of a Rotated couple Stress Rivlin Ericksen Ferro magnetic Fluid In Presence of Variable Gravity Field in a Porous Medium." *International Journal of Recent Scientific Research* 13, no. 05 (C) (2022): 1263-1276. <http://dx.doi.org/10.24327/ijrsr.2022.1305.0272>
- [25] Devi, Parasa Naga Lakshmi, and Phani Kumar Meduri. "Drag Over A Fluid Sphere Filled With Couple Stress Due to Flow of A Couple Stress Fluid with Slip Condition." *Trends in Sciences* 19, no. 24 (2022): 3133-3133. <https://doi.org/10.1002/zamm.202100340>
- [26] Devi, P. Naga Lakshmi, and Phani Kumar Meduri. "Couple stress fluid past a contaminated fluid sphere with slip condition." *Applied Mathematics and Computation* 446 (2023): 127845. <https://doi.org/10.1016/j.amc.2023.127845>
- [27] Palaiah, Suresha Suraiah, Hussain Basha, and Gudala Janardhana Reddy. "Magnetized couple stress fluid flow past a vertical cylinder under thermal radiation and viscous dissipation effects." *Nonlinear Engineering* 10, no. 1 (2021): 343-362. <https://doi.org/10.1515/nleng-2021-0027>
- [28] Kumar, Mahesh, Gudala Janardhana Reddy, Nedunuri Naresh Kumar, and Osman Anwar Bég. "Application of differential transform method to unsteady free convective heat transfer of a couple stress fluid over a stretching sheet." *Heat Transfer—Asian Research* 48, no. 2 (2019): 582-600. <https://doi.org/10.1002/htj.21396>
- [29] Muhammed, Rafeek KV, Hussain Basha, G. Janardhana Reddy, Usha Shankar, and O. Anwar Bég. "Influence of variable thermal conductivity and dissipation on magnetic Carreau fluid flow along a micro-cantilever sensor in a squeezing regime." *Waves in Random and Complex Media* (2022): 1-30. <https://doi.org/10.1080/17455030.2022.2139013>
- [30] Reddy, G. Janardhana, Mahesh Kumar, and H. P. Rani. "Study of entropy generation in transient hydromagnetic flow of couple stress fluid due to heat and mass transfer from a radiative vertical cylinder." *Pramana* 93 (2019): 1-14. <https://doi.org/10.1007/s12043-019-1861-9>
- [31] Reddy, G. Janardhana, Ashwini Hiremath, Mahesh Kumar, O. Anwar Bég, and Ali Kadir. "Unsteady magnetohydrodynamic couple stress fluid flow from a shrinking porous sheet: variational iteration method study." *Heat Transfer* 51, no. 2 (2022): 2219-2236. <https://doi.org/10.1002/htj.22397>
- [32] Basha, Hussain, G. Janardhana Reddy, NS Venkata Narayanan, and Mikhail A. Sheremet. "Analysis of supercritical free convection in Newtonian and couple stress fluids through EOS approach." *International Journal of Heat and Mass Transfer* 152 (2020): 119542. <https://doi.org/10.1016/j.ijheatmasstransfer.2020.119542>
- [33] V. K. Narla, Dharmendra Tripathi, and D.S. Bhandari. "Thermal analysis of micropolar fluid flow driven by electroosmosis and peristalsis in microchannels." *International Journal of Ambient Energy*, 43, (2022) no. 1. <https://doi.org/10.1080/01430750.2022.2091034>
- [34] Narla, V. K., Dharmendra Tripathi, D. S. Bhandari, and O. Anwar Bég. "Electrokinetic insect-bioinspired membrane pumping in a high aspect ratio bio-microfluidic system." *Microfluidics and Nanofluidics* 26, no. 11 (2022): 85. <http://dx.doi.org/10.1007/s10404-022-02588-2>
- [35] Akram, Javaria, Noreen Sher Akbar, Monairah Alansari, and Dharmendra Tripathi. "Electroosmotically modulated peristaltic propulsion of TiO₂/10W40 nanofluid in curved microchannel." *International Communications in Heat and Mass Transfer* 136 (2022): 106208. <https://doi.org/10.1016/j.icheatmasstransfer.2022.106208>
- [36] Akram, Javaria, Noreen Sher Akbar, and Dharmendra Tripathi. "Electroosmosis augmented MHD peristaltic transport of SWCNTs suspension in aqueous media." *Journal of Thermal Analysis and Calorimetry* (2022): 1-18.

- [37] Akram, Javaria, Noreen Sher Akbar, and Dharmendra Tripathi. "Analysis of electroosmotic flow of silver-water nanofluid regulated by peristalsis using two different approaches for nanofluid." *Journal of Computational Science* 62 (2022): 101696. <https://doi.org/10.1016/j.jocs.2022.101696>
- [38] Bhandari, D. S., and Dharmendra Tripathi. "Alteration in membrane-based pumping flow with rheological behaviour: A mathematical model." *Computer Methods and Programs in Biomedicine* 229 (2023): 107325. <http://dx.doi.org/10.1016/j.cmpb.2022.107325>
- [39] Bhandari, D. S., Dharmendra Tripathi, and O. Anwar Bég. "Electro-osmosis modulated periodic membrane pumping flow and particle motion with magnetic field effects." *Physics of Fluids* 34, no. 9 (2022): 092014. <https://doi.org/10.1063/5.0111050>
- [40] Bhandari, D. S., and Dharmendra Tripathi. "Study of entropy generation and heat flow through a microtube induced by the membrane-based thermofluidics systems." *Thermal Science and Engineering Progress* 34 (2022): 101395. <https://doi.org/10.1016/j.tsep.2022.101395>
- [41] Ram, Daya, D. S. Bhandari, Dharmendra Tripathi, and Kushal Sharma. "Propagation of H1N1 virus through saliva movement in oesophagus: a mathematical model." *The European Physical Journal Plus* 137, no. 7 (2022): 866. <https://doi.org/10.1140/epjp/s13360-022-03070-2>
- [42] Lu, D. C., S. Noreen, S. Waheed, and D. Tripathi. "Heat transfer applications in curved micro-channel driven by electroosmosis and peristaltic pumping." *Journal of Mechanics in Medicine and Biology* 22, no. 05 (2022): 2250030. <https://doi.org/10.1142/S0219519422500300>
- [43] Tripathi, Dharmendra, D. S. Bhandari, and O. Anwar Bég. "Thermal effects on SARS-CoV-2 transmission in peristaltic blood flow: mathematical modeling." *Physics of Fluids* 34, no. 6 (2022): 061904. <https://doi.org/10.1063/5.0095286>
- [44] Shaw, S., G. C. Shit, and D. Tripathi. "Impact of drug carrier shape, size, porosity and blood rheology on magnetic nanoparticle-based drug delivery in a microvessel." *Colloids and Surfaces A: Physicochemical and Engineering Aspects* 639 (2022): 128370. <https://doi.org/10.1016/j.colsurfa.2022.128370>